



Published in final edited form as:

Acad Radiol. 2005 September ; 12(9): 1121–1127.

Real-time, Interactive MRI for Cardiovascular Interventions¹

Elliot R. McVeigh, PhD, Michael A. Guttman, MS, Peter Kellman, PhD, Amish N. Raval, MD, and Robert J. Lederman, MD

From Laboratory of Cardiac Energetics (E.R.M., M.A.G., P.K.) and Cardiology Branch (A.N.R., R.J.L.), National Heart, Lung, and Blood Institute, National Institutes of Health, Building 10, Room B1D416, Bethesda, MD 20892-1061.

Keywords

MRI; intervention; real-time; therapy

Over the past decade, there has been a small contingent of laboratories developing magnetic resonance imaging (MRI)-guided intravascular techniques and applications. While these efforts have followed in the footsteps of MRI-guided surgical technologies (1,2), intravascular techniques do not carry the requirement for an open access scanner, and hence higher imaging performance during procedures can be achieved. The concept of precise real-time tracking of an active catheter in a standard MRI scanner was fully realized more than 15 years ago by Dumoulin and colleagues (3). Interventional MRI has subsequently developed into the obvious method for delivery of numerous therapies. This review addresses the recent developments and state-of-the-art of a number of aspects of interventional cardiovascular MRI.

REAL-TIME IMAGING

One of the principal enabling technologies for guiding intravascular procedures is real-time imaging. When catheter tracking was first implemented, special pulse sequences were required to obtain the catheter position from a few rapid projections; for some applications, this is now unnecessary due to the ability of modern scanners to provide up to 30 frames per second. There is obviously a tradeoff between spatial resolution and temporal resolution, but this is fully adjustable in an interactive system. One of the significant developments for real-time imaging is the use of multiple receiver systems used in conjunction with specially designed coil arrays to enable parallel imaging techniques. In this next section, some of these techniques are briefly described.

PARALLEL IMAGING METHODS

Parallel imaging is a rapid imaging method that can be applied to real-time imaging. Parallel imaging exploits the difference in sensitivity profiles between individual coil elements in a receive array to reduce the number of gradient encoding steps required for imaging. Parallel imaging uses R-fold k-space undersampling to achieve an acceleration factor of rate R. The alias artifacts (R uniformly spaced ghosts) caused by k-space undersampling are then cancelled by the parallel image reconstruction algorithm. Parallel image reconstruction may be performed in the k-space domain, for example, by using Simultaneous Acquisition of Spatial Harmonics (SMASH) (4), or in the image domain, for example, by using the sensitivity encoding method (SENSE) (5).

¹The authors are supported through the Intramural Research Program of the National Institutes of Health, Department of Health and Human Services.

Address correspondence to E.R.M. e-mail: emcveigh@nih.gov.

The acceleration factor is limited in practice by the available SNR and the ability to cancel the alias ghost images caused by undersampling. Parallel image reconstruction is based on solving a system of linear equations in the least-squares sense to separate the R-ghost alias images with signals from N receiver coils. The performance and robustness of the reconstruction algorithm are improved with $R \ll N$ (overdetermined set of equations). MR surface coil array and digital receiver technology have improved dramatically, and MR system products are now available with up to $N = 32$ channels, enabling robust performance with acceleration rate $R = 4$ in a single dimension.

The parallel imaging reconstruction assumes that the coil sensitivity profiles are known or can be estimated. A key area of current research has been on autocalibration methods for estimating the in vivo coil sensitivities (6-9). For real-time dynamic imaging applications, the adaptive TSENSE method (9) provides a means of automatic update which is useful for interventional MR application, which are free-breathing. In the TSENSE method, the k-space undersampling is varied cyclically in time such that after R-frames, all of k-space is acquired in a fashion similar to viewsharing or UNFOLD (10). Lower temporal resolution reference images may be reconstructed in order to calculate the coil sensitivities (B1 maps) used for parallel imaging solution. Parallel imaging image reconstruction has been implemented in real-time with low latency using a software-based multithreaded implementation (11).

Example real-time images acquired at approximately 30 fps with SENSE rate 4 are shown in Figure 1 (consecutive time frames). A true-FISP (SSFP) sequence provides high contrast between blood and myocardium. The imaging matrix in this example is 128×64 corresponding to $2.9 \times 5 \text{ m}^2$ in-plane spatial resolution for the specified FOV. The autocalibrating TSENSE method is used; imaging was performed using a 1.5-T Siemens Sonata with a custom eight-element linear array (Nova Medical, Inc., Wilmington, MA).

Real-time volumetric imaging of the entire heart was performed at 5 volumes per second using high acceleration rate parallel imaging. In three-dimensional imaging applications using two phase encode dimensions, it is preferable to perform accelerated imaging (k-space undersampling) in each of the two phase encode directions rather than a higher rate along a single direction. This has been referred to as 2D-SENSE (12). Example real-time, free-breathing volume images with a true-FISP sequence acquired at approximately 5 volumes per second with SENSE rate $4 \times 3 = 12$ are shown in Figure 2 (single volume). The imaging matrix in this example is $128 \times 54 \times 18$ corresponding to $2.5 \times 4.8 \times 8 \text{ m}^3$ resolution for the specified FOV. The autocalibrating TSENSE method is used; imaging was performed using a 32-channel 1.5-T Siemens Avanto with a prototype 32-element surface coil array from Rapid Biomedical (Wurzburg, Germany).

REAL-TIME INTERACTIVE SCANNER CONTROL

One of the uniquely useful features of MRI is that the image contrast, the imaging planes, and the spatial and temporal resolution can be changed interactively during imaging. Saturation pulses can be played between excitations, timings within the sequence can be altered, gradient amplitudes can be modified, or k-space trajectories can be changed. Image reconstruction and display can have many interactive features, ranging from changing reconstruction methods and parameters, to color highlighting, three-dimensional rendering, and device tracking.

The ability to change these imaging and display parameters during a scan may be used as the physician advances from one stage to another during an interventional procedure. For example, in a procedure requiring catheter-based delivery of a therapeutic agent to a precise target, one might start imaging with a large FOV as a catheter is navigated through the major vessels, color-highlight images using catheter coil signals, intermittently turn off slice selection to see the whole catheter (including portions that are outside the imaging plane), and then reduce the

FOV when nearing the target. Saturation or other contrast changes may be turned on to visualize delivery of the agent, and high-resolution images can be obtained to visualize the result of the delivery (ie, the shape of a burn or shape of an injection). Multiple imaging planes may be imaged and interactively adjusted during the scan to allow simultaneous views of the current catheter position and the target.

During the past several years, a number of research groups have developed systems that attach to an MR scanner and provide graphic user interfaces (GUIs) for real-time interactive imaging. The first of these systems allowed basic real-time imaging with a single adjustable imaging plane (13,14), then adding many of the features described earlier (15-19). More recently, there have been attempts to automate the changing of image parameters in response to motion of a device being tracked (20,21).

Some MR scanner manufacturers provide an interactive interface for adjusting imaging planes and some parameters during a real-time scan. These products also typically provide features for saving streams of images, book marking, pausing, and limited changes to image contrast, such as turning on a saturation pulse. In some cases, device tracking is also available.

Many of the research implementations use a high-performance computer attached to the MR scanner to obtain echo (or “raw”) data or reconstructed images as they become available. It is important to complete all image reconstructions and renderings no more than one-fourth second after the data are available; otherwise, manual tasks become increasingly difficult to perform using image guidance. Typically, a bus adapter or high-speed network connection is used for rapid data transfer. The computer can then perform reconstructions and graphic operations as necessary for the given procedure. Commands can also be sent from the computer to the scanner to “close the loop” and perform all scanner operations using custom software. One such implementation at the National Institutes of Health (22) uses a workstation with multiple 64-bit CPUs and high-performance graphics attached by gigabit Ethernet to the reconstruction computer of a Siemens Sonata or Avanto 1.5-T scanner. The displays of the MR scanner, external computer, and hemodynamic monitor are rear-projected in the magnet room as shown in Figure 3.

INTERVENTIONAL DEVICES

Passive Devices

Catheters can be located in the imaging volume using the contrast obtained from the distortion or loss of signal caused by the catheter (23); however, many things produce dark spots in MR images. If the imaging field of view containing the catheter is particularly cluttered, as is often the case in vascular areas around the heart, the device can be lost. Catheters filled with contrast agent such as Gd-DTPA can highlight the device with bright signal (24), but the device can still exit the imaging plane, causing the loss of the location of the tip. The principal advantage of passive devices is the fact that there is no concern about generating unwanted heating. A very successful application of a passive device is the CO₂-filled balloon used by Razavi and colleagues (25), which was also used by Kuehne and colleagues (26) to obtain right ventricular PV loops.

A recent passive device is a catheter filled with hyperpolarized C¹³ (27). While this requires a second transmit/receive system for the scanner (the resonant frequency of C¹³ is approximately one-fourth that of protons), the independent frequency is of great benefit in separating the device from the proton background image. In this way, it is conceivable that the device could be simultaneously imaged in a three-dimensional projection view, while simultaneous imaging of the tissue with protons.

Active Devices

Electrically connected devices—The concept of incorporating small locator coils into a catheter for tracking position, which was demonstrated more than a decade ago by Dumoulin and colleagues (3), has been well established (28).

Serfaty and colleagues (29) demonstrated that active guidewires could be used to position devices under MRI guidance and projection angiography could be performed (30), and recently Omary and colleagues (31) demonstrated performing coronary catheterization on 12 of 12 swine with an active guidewire.

A Stelleto (Boston Scientific, Natick, MA) injection catheter has been modified to act as two separate coils: one in the shaft of the catheter, and the other localized to the tip. These two coils can be connected to their own channels in the receiver. This device was used to target the injection of mesenchymal stem cells in the border zone of infarcts (32). A similar injection catheter design has been implemented by Karmarkar and colleagues (33). Zuehlsdorff and colleagues (34) made an active catheter with the ability to switch between a set of loops on the shaft of a catheter and a single small coil located at the tip.

Safety is an issue with any device that is electrically active; a considerable effort has been focused on the potential of conducting devices to generate unwanted heating in the tissue (35-43). For widespread use in humans, electrically active devices will need to incorporate cables in which the currents are eliminated by radiofrequency (RF) chokes incorporated into the cable (44,45).

Inductively coupled devices—Quick and colleagues (46) implemented a catheter device in which a resonant coil is imbedded, but this coil is not electronically connected to the scanner. The signal amplitude is amplified around the imbedded coil by inductive coupling between the imbedded coil and the receiver coil on the body surface. Also, the effective tip angle around the imbedded coil is amplified, causing very bright signal for low tip angle images. These devices do not need to be connected to a receiver, so there is no need to have a connector on the proximal end of the catheter; this makes it simpler.

INTERVENTIONAL PROCEDURES

A host of applications are currently being developed with real-time MRI guidance; this section lists a few of these applications.

Real-time display of the catheter position on three-dimensional MRI has been shown to be useful for anatomically targeted catheter navigation and subsequent RF ablation in the inferior vena cava, the fossa ovalis, and the left atrium (47). Preliminary catheter tracking with acquisition of filtered local electrograms has been reported (37), as has MRI characterization of ablated myocardium (48). The use of real-time interactive MRI for full real-time guidance of these procedures will also allow the physician to monitor the size of the lesion immediately after RF application. This will make the procedure faster and safer.

Schalla and colleagues (49) demonstrated transvenous and transarterial cardiac catheterization in a porcine model of atrial septal defect wholly using SSFP rtMRI and tracking receiver microcoils to mark the catheter tips.

Percutaneous transcatheter myocardial injection of gadolinium injectate (50) and the targeted delivery of iron-labeled mesenchymal stem cells to specific myocardial infarct targets (32) have both been reported. These injection applications used multiple active intravascular devices with three-dimensional volume rendering of multislice acquisitions, with color-

highlighting of catheter-related signal. Also, retrograde transaortic access has been used to perform image-guided myocardial injections (33,51).

MRI-guided transcatheter aortic valve replacement in swine using passive nitinol devices was achieved by Kuehne and colleagues (26). This application is attractive because of the critical importance of image-guided placement of the stent-valve in relation to the coronary arteries and aortic root.

Several groups (52,53) performed percutaneous coronary artery intervention in healthy animals and demonstrated images of intracoronary stent artifacts (52).

EXTRACARDIAC

Several groups have conducted angioplasty (54-58) and stenting (59-63) (Telep, unpublished data, 2004) using passive and active catheter techniques in animal models of arterial stenosis. Also, aortic aneurysm endografts (64,65) and inferior vena cava filter (66-68) devices have been placed, and embolization of renal artery segments (69,70) has been achieved.

Recently, Ravel and colleagues (71) recanalized long segments of chronic total arterial occlusions in an animal model. Using a custom catheter and guidewire coils, they were able to traverse long segments of occlusion while keeping within arterial adventitial borders, an important clinical challenge. Weiss and colleagues (45) made a transcatheter “mesocaval shunt,” or extrahepatic connection between portal and venous circulations, first using a septostomy needle and later using a novel custom vascular connector. Kee and colleagues integrated a flat-panel XRF system in a double-doughnut operative MRI system and conducted multimodal transjugular intrahepatic portosystemic shunting (TIPS) in animals (72) and in patients (73), showed a significant reduction in number of punctures required.

EARLY HUMAN EXPERIENCE

A few human rtMRI procedures have been conducted. Razavi and colleagues (25) reported a landmark series of cardiac catheterization performed successfully in children using a combined XMR environment. The Regensburg team conducted high-quality selective intra-arterial MR angiography (74) and reported some preliminary revascularization procedures using passive devices in the iliac (23) and femoral (74) arteries. As described earlier, the Stanford team has conducted rtMRI-assisted TIPS procedures in patients (73).

FUTURE DIRECTIONS

The procedures that will benefit the most from MRI guidance are those that are improved by immediate visualization of the effect of treatment. This is particularly obvious for ablation techniques, targeted injections, and vascular treatments in which the nature of the flow in a vessel is vital information. The technologies that are in critical need at this time are catheter-based instrumentation which is MRI compatible. To date, there has been little interest from catheter manufacturers in developing these tools for the simple reason that they will not sell very many in the next few years. This means that demonstration of the benefits from these technologies and procedures will be principally due to the efforts of independent laboratories.

REFERENCES

1. Jolesz FA, Talos IF, Schwartz RB, et al. Intraoperative magnetic resonance imaging and magnetic resonance imaging-guided therapy for brain tumors. *Neuroimaging Clin N Am* 2002;12:665–683. [PubMed: 12687918]

2. Schulz T, Puccini S, Schneider JP, Kahn T. Interventional and intraoperative MR: Review and update of techniques and clinical experience. *Eur Radiol.* 2004
3. Dumoulin CL, Souza SP, Darrow RD. Real-time position monitoring of invasive devices using magnetic resonance. *Magn Reson Med* 1993;29:411–415. [PubMed: 8450752]
4. Sodickson DK, Manning WJ. Simultaneous acquisition of spatial harmonics (SMASH): Fast imaging with radiofrequency coil arrays. *Magn Reson Med* 1997;38:591–603. [PubMed: 9324327]
5. Pruessmann KP, Weiger M, Scheidegger MB, Boesiger P. SENSE: Sensitivity encoding for fast MRI. *Magn Reson Med* 1999;42:952–962. [PubMed: 10542355]
6. Jakob PM, Griswold MA, Edelman RR, Sodickson DK. AUTO-SMASH: a self-calibrating technique for SMASH imaging. *SiMultaneous Acquisition of Spatial Harmonics. MAGMA* 1998;7:42–54. [PubMed: 9877459]
7. Griswold MA, Jakob PM, Heidemann RM, et al. Generalized autocalibrating partially parallel acquisitions (GRAPPA). *Magn Reson Med* 2002;47:1202–1210. [PubMed: 12111967]
8. McKenzie CA, Yeh EN, Ohliger MA, et al. Self-calibrating parallel imaging with automatic coil sensitivity extraction. *Magn Reson Med* 2002;47:529–538. [PubMed: 11870840]
9. Kellman P, Epstein FH, McVeigh ER. Adaptive sensitivity encoding incorporating temporal filtering (TSENSE). *Magn Reson Med* 2001;45:846–852. [PubMed: 11323811]
10. Madore B, Glover GH, Pelc NJ. Unaliasing by Fourier-encoding the overlaps using the temporal dimension (UNFOLD), applied to cardiac imaging and fMRI. *Magn Reson Med* 1999;42:813–828. [PubMed: 10542340]
11. Guttman MA, Kellman P, Dick AJ, et al. Real-time accelerated interactive MRI with adaptive TSENSE and UNFOLD. *Magn Reson Med* 2003;50:315–321. [PubMed: 12876708]
12. Weiger M, Pruessmann KP, Osterbauer R, et al. Sensitivity-encoded single-shot spiral imaging for reduced susceptibility artifacts in BOLD fMRI. *Magn Reson Med* 2002;48:860–866. [PubMed: 12418001]
13. Holsinger AE, Wright RC, Siederer SJ, et al. Real-time interactive magnetic resonance imaging. *Magn.Reson.Med* 1990;14:547–553. [PubMed: 2355836]
14. Kerr, A.; Pauly, J.; Hu, B., et al. International Society for Magnetic Resonance in Medicine, Book of Abstracts. 1. 1997. Real-time interactive MRI on a conventional scanner; p. 319
15. Nayak KS, Pauly JM, Yang PC, et al. Real-time interactive coronary MRA. *Magn Reson Med* 2001;46:430–435. [PubMed: 11550232]
16. Aksit P, Derbyshire JA, Serfaty JM, Atalar E. Multiple field of view MR fluoroscopy. *Magn Reson Med* 2002;47:53–60. [PubMed: 11754442]
17. Guttman MA, Lederman RJ, Sorger JM, McVeigh ER. Real-time volume rendered MRI for interventional guidance. *J Cardiovasc Magn Reson* 2002;4:431–442. [PubMed: 12549231]
18. Quick HH, Kuehl H, Kaiser G, et al. Interventional MR angiography with a floating table. *Radiology* 2003;229:598–602. [PubMed: 14500852]
19. Nayak KS, Cunningham CH, Santos JM, Pauly JM. Real-time cardiac MRI at 3 Tesla. *Magn Reson Med* 2004;51:655–660. [PubMed: 15065236]
20. Elgort DR, Wong EY, Hillenbrand CM, et al. Real-time catheter tracking and adaptive imaging. *J Magn Reson Imaging* 2003;18:621–626. [PubMed: 14579407]
21. Bock M, Volz S, Zuhlsdorff S, et al. MR-guided intravascular procedures: Real-time parameter control and automated slice positioning with active tracking coils. *J Magn Reson Imaging* 2004;19:580–589. [PubMed: 15112307]
22. Guttman MA, Dick AJ, Raman VK, et al. Imaging of myocardial infarction for diagnosis and intervention using real-time interactive MRI without ECG-gating or breath-holding. *Magn Reson Med* 2004;52:354–361. [PubMed: 15282818]
23. Manke C, Nitz WR, Djavidani B, et al. MR imaging-guided stent placement in iliac arterial stenoses: A feasibility study. *Radiology* 2001;219:527–534. [PubMed: 11323483]
24. Unal O, Korosec FR, Frayne R, et al. A rapid 2D time-resolved variable-rate k-space sampling MR technique for passive catheter tracking during endovascular procedures. *Magn Reson Med* 1998;40:356–362. [PubMed: 9727937]

25. Razavi R, Hill DL, Keevil SF, et al. Cardiac catheterisation guided by MRI in children and adults with congenital heart disease. *Lancet* 2003;362:1877–1882. [PubMed: 14667742]
26. Kuehne T, Yilmaz S, Steendijk P, et al. Magnetic resonance imaging analysis of right ventricular pressure-volume loops: In vivo validation and clinical application in patients with pulmonary hypertension. *Circulation* 2004;110:2010–2016. [PubMed: 15451801]
27. Svensson J, Mansson S, Johansson E, et al. Hyperpolarized ¹³C MR angiography using true FISP. *Magn Reson Med* 2003;50:256–262. [PubMed: 12876701]
28. Wildermuth S, Debatin JF, Leung DA, et al. MR imaging-guided intravascular procedures: Initial demonstration in a pig model. *Radiology* 1997;202:578–583. [PubMed: 9015094]
29. Serfaty JM, Yang X, Aksit P, et al. Toward MRI-guided coronary catheterization: Visualization of guiding catheters, guidewires, and anatomy in real time. *J Magn Reson Imaging* 2000;12:590–594. [PubMed: 11042641]
30. Serfaty JM, Atalar E, Declerck J, et al. Real-time projection MR angiography: Feasibility study. *Radiology* 2000;217:290–295. [PubMed: 11012459]
31. Omary RA, Green JD, Schirf BE, et al. Real-time magnetic resonance imaging-guided coronary catheterization in swine. *Circulation* 2003;107:2656–2659. [PubMed: 12756160]
32. Dick AJ, Guttman MA, Raman VK, et al. Magnetic resonance fluoroscopy enables targeted delivery of mesenchymal stem cells to infarct borders in swine. *Circulation* 2003;108:2899–2904. [PubMed: 14656911]
33. Karmarkar PV, Kraitchman DL, Izbudak I, et al. MR-trackable intramyocardial injection catheter. *Magn Reson Med* 2004;51:1163–1172. [PubMed: 15170836]
34. Zuehlsdorff S, Umatham R, Volz S, et al. MR coil design for simultaneous tip tracking and curvature delineation of a catheter. *Magn Reson Med* 2004;52:214–218. [PubMed: 15236390]
35. Qiu B, Yeung CJ, Du X, et al. Development of an intravascular heating source using an MR imaging guidewire. *J Magn Reson Imaging* 2002;16:716–720. [PubMed: 12451585]
36. Quick HH, Serfaty JM, Pannu HK, et al. Endourethral MRI. *Magn Reson Med* 2001;45:138–146. [PubMed: 11146495]
37. Susil RC, Yeung CJ, Halperin HR, et al. Multifunctional interventional devices for MRI: A combined electrophysiology/MRI catheter. *Magn Reson Med* 2002;47:594–600. [PubMed: 11870847]
38. Yang X, Yeung CJ, Ji H, et al. Thermal effect of intravascular MR imaging using an MR imaging-guidewire: An in vivo laboratory and histopathological evaluation. *Med Sci Monit* 2002;8:MT113–MT117. [PubMed: 12118208]
39. Yeung CJ, Atalar E. RF transmit power limit for the barewire loopless catheter antenna. *J Magn Reson Imaging* 2000;12:86–91. [PubMed: 10931568]
40. Yeung CJ, Atalar E. A Green's function approach to local RF heating in interventional MRI. *Med Phys* 2001;28:826–832. [PubMed: 11393478]
41. Yeung CJ, Susil RC, Atalar E. RF heating due to conductive wires during MRI depends on the phase distribution of the transmit field. *Magn Reson Med* 2002;48:1096–1098. [PubMed: 12465125]
42. Yeung CJ, Susil RC, Atalar E. RF safety of wires in interventional MRI: Using a safety index. *Magn Reson Med* 2002;47:187–193. [PubMed: 11754458]
43. Armenean C, Perrin E, Armenean M, et al. RF-induced temperature elevation along metallic wires in clinical magnetic resonance imaging: Influence of diameter and length. *Magn Reson Med* 2004;52:1200–1206. [PubMed: 15508156]
44. Atalar, E.; Ocali, O. Enhanced safety coax cables. United States; Apr 9. 2001
45. Weiss, C.; Arepally, A.; Karmarkar, PV.; Atalar, E. Proceedings of the Twelfth Annual ISMRM. 962. ISMRM; Berkley, CA: 2004. Real-time MR-guided meso-caval puncture: Towards the development of a Percutaneous MR-guided mesocaval shunt.
46. Quick HH, Kuehl H, Kaiser G, et al. Inductively coupled stent antennas in MRI. *Magn Reson Med* 2002;48:781–790. [PubMed: 12417992]
47. Dickfeld T, Calkins H, Zviman M, et al. Stereotactic magnetic resonance guidance for anatomically targeted ablations of the fossa ovalis and the left atrium. *J Interv Card Electrophysiol* 2004;11:105–115. [PubMed: 15383773]

48. Lardo AC, McVeigh ER, Jumrussirikul P, et al. Visualization and temporal/spatial characterization of cardiac radiofrequency ablation lesions using magnetic resonance imaging. *Circulation* 2000;102:698–705. [PubMed: 10931812]
49. Schalla S, Saeed M, Higgins CB, et al. Magnetic resonance-guided cardiac catheterization in a swine model of atrial septal defect. *Circulation* 2003;108:1865–1870. [PubMed: 14517162]
50. Lederman RJ, Guttman MA, Peters DC, et al. Catheter-based endomyocardial injection with real-time magnetic resonance imaging. *Circulation* 2002;105:1282–1284. [PubMed: 11901036]
51. Saeed M, Lee R, Martin A, et al. Transendocardial delivery of extracellular myocardial markers by using combination X-ray/MR fluoroscopic guidance: Feasibility study in dogs. *Radiology* 2004;231:689–696. [PubMed: 15163809]
52. Spuentrup E, Ruebben A, Schaeffter T, et al. Magnetic resonance-guided coronary artery stent placement in a swine model. *Circulation* 2002;105:874–879. [PubMed: 11854130]
53. Serfaty JM, Yang X, Foo TK, et al. MRI-guided coronary catheterization and PTCA: A feasibility study on a dog model. *Magn Reson Med* 2003;49:258–263. [PubMed: 12541245]
54. Wildermuth S, Dumoulin CL, Pfammatter T, et al. MR-guided percutaneous angioplasty: Assessment of tracking safety, catheter handling and functionality. *Cardiovasc Interv Radiol* 1998;21:404–410.
55. Yang X, Bolster BD, Kraitchman DL, Atalar E. Intravascular MR-monitored balloon angioplasty: An in vivo feasibility study. *J Vasc Interv Radiol* 1998;9:953–959. [PubMed: 9840040]
56. Buecker A, Adam GB, Neuerburg JM, et al. Simultaneous real-time visualization of the catheter tip and vascular anatomy for MR-guided PTA of iliac arteries in an animal model. *J Magn Reson Imaging* 2002;16:201–208. [PubMed: 12203769]
57. Godart F, Beregi JP, Nicol L, et al. MR-guided balloon angioplasty of stenosed aorta: In vivo evaluation using near-standard instruments and a passive tracking technique. *J Magn Reson Imaging* 2000;12:639–644. [PubMed: 11042648]
58. Omary RA, Unal O, Koscielski DS, et al. Real-time MR imaging-guided passive catheter tracking with use of gadolinium-filled catheters. *J Vasc Interv Radiol* 2000;11:1079–1085. [PubMed: 10997475]
59. Buecker A, Neuerburg JM, Adam GB, et al. Real-time MR fluoroscopy for MR-guided iliac artery stent placement. *J Magn Reson Imaging* 2000;12:616–622. [PubMed: 11042645]
60. Dion YM, Ben El KH, Boudoux C, et al. Endovascular procedures under near-real-time magnetic resonance imaging guidance: An experimental feasibility study. *J Vasc Surg* 2000;32:1006–1014. [PubMed: 11054233]
61. Quick HH, Ladd ME, Hoevel M, et al. Real-time MRI of joint movement with true FISP. *J Magn Reson Imaging* 2002;15:710–715. [PubMed: 12112522]
62. Kivelitz D, Wagner S, Schnorr J, et al. A vascular stent as an active component for locally enhanced magnetic resonance imaging: Initial in vivo imaging results after catheter-guided placement in rabbits. *Invest Radiol* 2003;38:147–152. [PubMed: 12595794]
63. Kuehne T, Saeed M, Higgins CB, et al. Endovascular stents in pulmonary valve and artery in swine: Feasibility study of MR imaging-guided deployment and postinterventional assessment. *Radiology* 2003;226:475–481. [PubMed: 12563142]
64. Mahnken AH, Chalabi K, Jalali F, et al. Magnetic resonance-guided placement of aortic stents grafts: Feasibility with real-time magnetic resonance fluoroscopy. *J Vasc Interv Radiol* 2004;15:189–195. [PubMed: 14963188]
65. Raman VK, Karmarkar PV, Guttman MA, et al. Real-time magnetic resonance-guided endovascular repair of experimental abdominal aortic aneurysm in Swine. *J Am Coll Card* 2005;45:2069–2077.
66. Frahm C, Gehl HB, Lorch H, et al. MR-guided placement of a temporary vena cava filter: Technique and feasibility. *J Magn Reson Imaging* 1998;8:105–109. [PubMed: 9500268]
67. Bartels LW, Bos C, van der WR, et al. Placement of an inferior vena cava filter in a pig guided by high-resolution MR fluoroscopy at 1.5 T. *J Magn Reson Imaging* 2000;12:599–605. [PubMed: 11042643]
68. Bucker A, Neuerburg JM, Adam GB, et al. Real-time MR guidance for inferior vena cava filter placement in an animal model. *J Vasc Interv Radiol* 2001;12:753–756. [PubMed: 11389228]
69. Bucker A, Neuerburg JM, Adam G, et al. MR-guided coil embolisation of renal arteries in an animal model. *Rof* 2003;175:271–274. [PubMed: 12584630]

70. Fink C, Bock M, Umatham R, et al. Renal embolization: Feasibility of magnetic resonance-guidance using active catheter tracking and intraarterial magnetic resonance angiography. *Invest Radiol* 2004;39:111–119. [PubMed: 14734926]
71. Raval AN, Karmarkar PV, Ozturk C, et al. Chronic total peripheral artery occlusion recanalization using interactive real-time magnetic resonance imaging guidance is feasible in a swine model [abstract]. *J Cardiovasc Magn Reson* 2005:65.
72. Kee ST, Ganguly A, Daniel BL, et al. MR-guided transjugular intrahepatic portosystemic shunt creation with use of a hybrid radiography/MR system. *J Vasc Interv Radiol* 2005;16(2 Pt 1):227–234. [PubMed: 15713923]
73. Butts K. MRI-guided TIPS procedures in man. 2004
74. Paetzel C, Zorger N, Bachthaler M, et al. Feasibility of MR-guided angioplasty of femoral artery stenoses using real-time imaging and intraarterial contrast-enhanced MR angiography. *Rofo* 2004;176:1232–1236. [PubMed: 15346256]

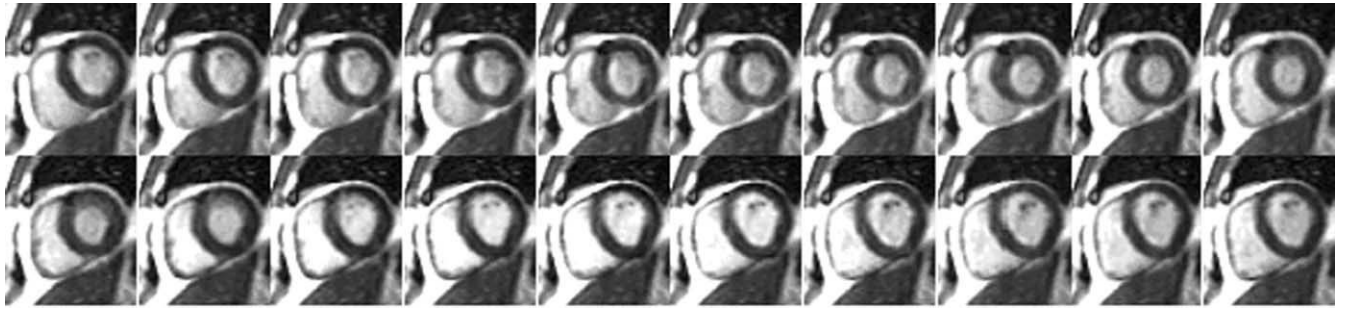


Figure 1.
Example real-time images of short axis slice using rate $R = 4$ SENSE at 30 frames per second.

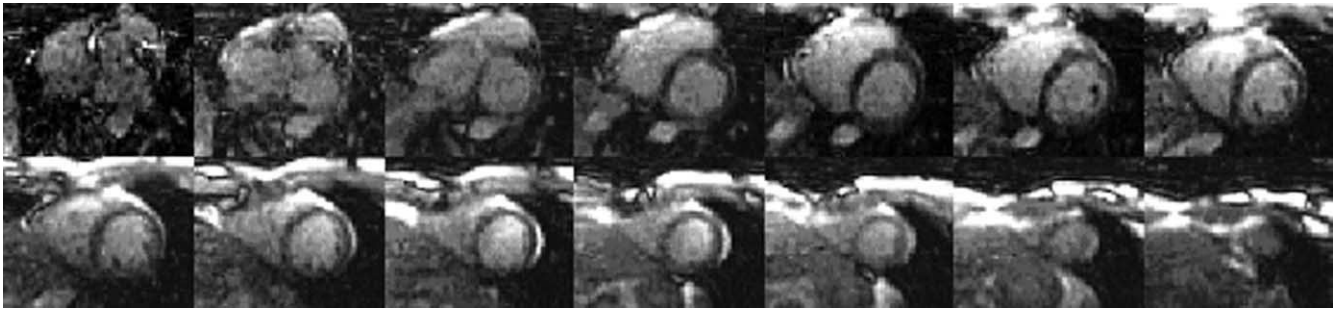
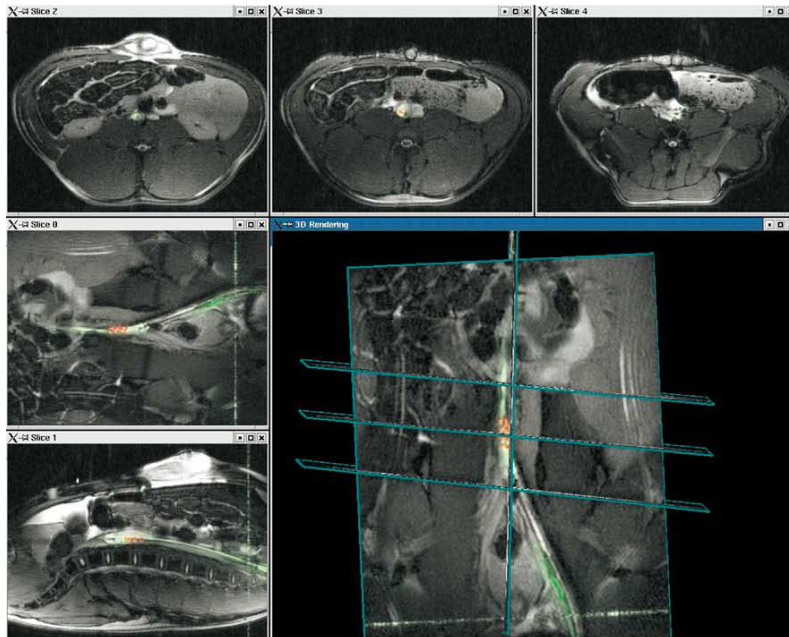


Figure 2.
Example real-time volumetric images for a single time frame using rate $R = 4 \times 3$ SENSE at 5 volumes per seconds.



a.



b.

Figure 3. (a) Picture during an interventional procedure at the National Institutes of Health (NIH). The rear projection screen shows monitors from the MR scanner, an external computer, and the hemodynamics monitor. (b) Real-time multiple slice imaging with active invasive devices and three-dimensional rendering on the custom reconstruction computer at the NIH. Procedure shown is experimental placement of an endograft in an abdominal aortic aneurysm in a pig. Image data from coils in the guiding catheter are highlighted green; image data from coils just distal to the endograft are highlighted red.